Electrochemistry of Late Transition Metal Complexes Containing the Ligand 1,1′-Bis(diisopropylphosphino)ferrocene (dippf)[#]

Joyce H. L. Ong,[†] Chip Nataro,*[,†] James A. Golen,[‡,§,⊥] and Arnold L. Rheingold[‡,§]

Department of Chemistry, Lafayette College, Easton, Pennsylvania 18042, and Department of Chemistry & Biochemistry, University of Delaware, Newark, Delaware 19716

Received July 2, 2003

The chemically reversible oxidation of 1,1′-bis(diisopropylphosphino)ferrocene (dippf) was investigated using cyclic voltammetry. In addition, seven new compounds with general formulas of $[(MCl_n)_m(dippf)]$ (M = Co, Ni, Pt, Zn, Cd or Hg, $n = 2$, $m = 1$; M = Au, $n = 1$, $m = 2$) have been prepared. The Ni and Co compounds were found to be paramagnetic, and the Evans method was used to determine the magnetic moment for these compounds. The remaining compounds were characterized by ^{1}H, ^{13}C, and ^{31}P NMR. As an additional means of characterization, the molecular structures of $[PtCl_2(dippf)]$ and $[ZnCl_2(dippf)]$ were determined. The electrochemistry of the new compounds and the previously synthesized $[PdCl_2(dippf)]$ was investigated using cyclic voltammetry. The results of this investigation show that coordination of the dippf ligands leads to more positive oxidation potentials for the ferrocene backbone.

Introduction

Although both are commercially available, 1,1′-bis(diphenylphospino)ferrocene (dppf)[1] has been studied more thoroughly than the analogous isopropyl compound, 1,1′-bis(diisopropylphosphino)ferrocene (dippf). One means of evaluating this difference is to look at the number of reported structures that contain either of these phosphines. At the time of this report, there are approximately 320 structures containing dppf registered in the Cambridge Crystallographic Data Centre, while there are only 13 structures containing dippf. The structure of dippf has apparently been determined, but not yet reported.[2] Of the 13 published dippf-containing structures, three are of the phosphine chalcogenides, $dippfE_2$ (E = O, S, or Se).[3] One structure has $dippfS_2$ bridging two Te centers.[4] Of the remaining structures, six have dippf coordinated to a square-planar Pd(II) center.[5]

Many of the reports of compounds containing dippf have focused on catalytic processes, particularly using Pd(II) catalysts. For the cooligomerization of butadiene and carbon monoxide in the presence of $Pd(acac)_2$, dippf was found to be far superior to dppf in selectivity.[5b] In the catalysis of the Heck reaction, $[PdCl_2(dippf)]$ was determined to be a superior catalyst to the analogous dppf compound.[5a] However, in hydroamination reactions using Pd(II) catalysts, higher yields were obtained using dppf as a ligand for the catalyst as compared to dippf.[5f] Steric and electronic properties are often cited as the reasons for the variation in activity of dppf and dippf. However, compounds containing dppf and dippf have been compared only sterically.[6]

It is surprising that the electronic nature of dippf has not been investigated. Since dippf contains a redox-active ferrocene backbone, studying the electrochemistry of dippf may provide insight into its electronic nature. The electrochemistry of dppf has been thoroughly studied, and, unlike ferrocene, the oxidation is complicated by a chemical follow-up reaction.[7] However, upon coordination, the oxidation of dppf is frequently but not always reversible.[8] The property that seems to govern the reversibility of the oxidation of dppf is the lone pair of electrons on the phosphorus atoms. If the phosphorus atoms are strongly bound to a metal center such as $[PdCl_2(dppf)]$ or oxidized to phosphorus(V) as in $dppfO_2$,

[#] Presented in part at the 226th National Meeting of the American Chemical Society, New York, NY, September 7−11, 2003; see: *Abstracts of Papers*, INOR 409.

* Corresponding author. E-mail: nataroc@lafayette.edu.
[†] Lafayette College.
[‡] University of Delaware.
[§] Current address: Department of Chemistry and Biochemistry, University of San Diego, La Jolla, CA 92093.
[⊥] Permanent address: Department of Chemistry and Biochemistry, University of Massachusetts Dartmouth, North Dartmouth, MA 02747.

(1) Gan, K.-S.; Hor, T. S. A. *In Ferrocenes. From Homogeneous Catalysis to Material Science*; Togni, A., Hayashi, T., Eds.; VCH: New York, 1995; p 3.
(2) Elsagir, A. R.; Gassner, F.; Gorls, H.; Dinjus, E. *J. Organomet. Chem.* **2000**, *597*, 139. Ref 8 makes note of the dippf structure, but it has yet to be published.
(3) Necas, M.; Beran, M.; Woolins, J. D.; Novosad, J. *Polyhedron* **2001**, *20*, 741.
(4) Necas, M.; Novosad, J.; Husebye, S. *J. Organomet. Chem.* **2001**, *623*, 124.
(5) (a) Boyes, A. L.; Butler, I. R.; Quayle, S. C. *Tetrahedron Lett.* **1998**, *39*, 7763. (b) Elsagir, A. R.; Gassner, F.; Gorls, H.; Dinjus, E. *J. Organomet. Chem.* **2000**, *597*, 139. (c) Guzei, I. A.; Maisela, L. L.; Darkwa, J. *Acta Crystallogr. Sect. C: Cryst. Struct. Commun.* **2000**, *56*, 564. (d) Maisela, L. L.; Crouch, A. N.; Darkwa, J.; Guzei, I. A. *Polyhedron* **2001**, *20*, 3189. (e) Culkin, D. A.; Hartwig, J. F. *J. Am. Chem. Soc.* **2002**, *124*, 9330. (f) Kelin, L.; Horton, P. N.; Hursthouse, M. B.; Hii, K. K. *J. Organomet. Chem.* **2003**, *665*, 250.
(6) Avent, A. G.; Bedford, R. B.; Chaloner, P. A.; Dewa, S. Z.; Hitchcock, P. B. *J. Chem. Soc., Dalton Trans.* **1996**, 4633.
(7) (a) Pilloni, G.; Longato, B.; Corain, B. *J. Organomet. Chem.* **1991**, *420*, 57. (b) Nataro, C.; Campbell, A. N.; Ferguson, M. A.; Incarvito, C. D.; Rheingold, A. L. *J. Organomet. Chem.* **2003**, *673*, 47.
(8) Corain, B.; Longato, B.; Favero, G.; Ajò, D.; Pilloni, G.; Russo, U.; Kreissl, F. R. *Inorg. Chim. Acta* **1989**, *157*, 259.

10.1021/om0340138 CCC: $25.00
Publication on Web 10/31/2003

the oxidation is typically reversible.[8] However, if the phosphorus atoms are weakly bound such as [$ZnCl_2$-(dppf)] or noncoordinated, the product of the oxidation either decomposes or undergoes a more complex chemical step.[8]

In this study, we report the oxidative electrochemistry of dippf. In addition, the syntheses and characterization of seven new compounds containing dippf are reported. The X-ray structures of two of the new compounds were determined and compared to related dippf- and dppf-containing compounds. Additionally, the new compounds and a previously reported compound of dippf were investigated electrochemically.

Experimental Section

General Procedures. Preparative reactions and purifications were carried out using standard Schlenk techniques under an atmosphere of argon. Solvents were purified under nitrogen using standard methods. Hexanes, chloroform, and methylene chloride (DCM) were refluxed over CaH_2 and then distilled. Diethyl ether was distilled over potassium benzophenone ketyl. Reagent grade methanol, ethanol, and 2-propanol were used without additional purification. Electrochemical experiments were performed in HPLC grade DCM from Aldrich, which was distilled from CaH_2 under argon prior to use. The NMR data were obtained in $CDCl_3$ using a JEOL Eclipse 400 FT-NMR. The internal standard for ^1H and ^{13}C NMR acquisitions was TMS ($\delta = 0.00$ ppm). The $^{31}P\{^1H\}$ NMR data are referenced versus an external standard, 85% H_3PO_4. Elemental analyses were performed by Quantitative Technologies, Inc.

Ferrocene, decamethylferrocene, and dippf were purchased from Strem. Ferrocene was sublimed prior to use. Tetrabutylammonium hexaflurophosphate ($[NBu_4]^+[PF_6]^-$) was purchased from Aldrich and dried in vacuo prior to use. Li-$[B(C_6F_5)_4]\cdot(OEt_2)_{2.5}$ was purchased from Boulder Scientific Co. and metathesized to tetrabutylammonium tetrakis(pentafluorophenyl)borate ($[NBu_4]^+[B(C_6F_5)_4]^-$) according to the literature procedure.[9]

Synthesis. [$NiCl_2$(dippf)] (1). $NiCl_2\cdot 6H_2O$ (0.0998 g, 0.42 mmol) was dissolved in 3.5 mL of a mixture of 2-propanol−methanol (5:2 v/v). A solution of dippf (0.15 g, 0.37 mmol) in warm 2-propanol (4 mL) was added. The reaction was stirred for 30 min in a hot water bath, during which time a green precipitate formed. The solution was filtered, and the solid was washed with ether (2 × 5 mL) and dried under vacuum, giving **1** as a dark green powder (0.12 g, 59%). Anal. Calcd for $C_{22}H_{36}Cl_2FeNiP_2$: C, 48.23; H, 6.62. Found: C, 47.88; H, 6.66. UV−vis (DCM, λ nm, ϵ L/(cm·mol)): 390 (2830), 606 (304), 837 (194).

[$PdCl_2$(dippf)] (2). 2 was prepared according to the literature procedure.[2]

[$PtCl_2$(dippf)] (3). A mixture of $[PtCl_2(CH_3CN)_2]$ (0.0703 g, 0.20 mmol) and dippf (0.0841 g, 0.20 mmol) in 20 mL of DCM was stirred at room temperature for 1 h. The solution was concentrated under vacuum to ca. 5 mL, then 5 mL of DCM and 20 mL of hexanes were added to precipitate a yellow powder. The solution was filtered, washed with ether (2 × 5 mL), and dried under vacuum to afford **3** as a yellow powder (0.044 g, 32%). Crystals of **3** were obtained by dissolving in minimal DCM, layering with Et_2O, and slowly cooling in a freezer. Anal. Calcd for $C_{22}H_{36}Cl_2FeP_2Pt$: C, 38.61; H, 5.30. Found: C, 38.37; H, 5.05. $^{31}P\{^1H\}$ NMR ($CDCl_3$): δ 30.73 (s, $^1J_{P-Pt} = 3800$ Hz). ^1H NMR ($CDCl_3$): δ 4.49 (s, 4H, Cp), 4.44 (s, 4H, C_5H_4), 2.99 (dsept, $^3J_{H-H} = 7.32$ Hz, $^2J_{H-P} = 2.56$ Hz, 4H, $-CHMe_2$), 1.54 (dd, $^3J_{H-H} = 6.96$ Hz, $^3J_{H-P} = 16.84$ Hz, 12H, $-CH_3$), 1.17 (dd, $^3J_{H-H} = 6.96$ Hz, $^3J_{H-P} = 15.74$ Hz, 12H, $-CH_3$). $^{13}C\{^1H\}$ ($CDCl_3$): δ 73.27 (s), 72.81 (s), 72.21 (s), 26.93 (d, $^1J_{C-P} = 39.2$ Hz), 20.24 (s), 19.33 (s).

[$CoCl_2$(dippf)] (4). $CoCl_2\cdot 2H_2O$ (0.1659 g, 1.00 mmol) was dissolved in 4.0 mL of a mixture of 2-propanol−methanol (2:1 v/v). A solution of dippf (0.418 g, 1.00 mmol) in warm 2-propanol (40 mL) was added. The resulting dark blue solution was refluxed for 2 h, during which time a green precipitate formed. The solution was filtered, and the solid was washed with ether (2 × 5 mL) and dried under vacuum, giving **4** as a dark blue powder (0.262 g, 46%). Anal. Calcd for $C_{22}H_{36}Cl_2CoFeP_2$: C, 48.21; H, 6.62. Found: C, 48.16; H, 6.67. UV−vis (DCM, λ nm, ϵ L/(cm·mol)): 465 (264), 606 (388), 638 (600), 727 (464).

[$ZnCl_2$(dippf)] (5). $ZnCl_2$ (0.14 g, 1.0 mmol) was dissolved in 2.0 mL of a 2:1 v/v mixture of 2-propanol−methanol. A solution of dippf (0.42 g, 1.0 mmol) in warm 2-propanol (40 mL) was added. The resulting solution was refluxed for 2 h, during which time an orange precipitate formed. The solution was filtered, and the solid was washed with ether (2 × 5 mL) and dried under vacuum to afford **5** as an orange powder (0.18 g, 32%). Crystals of **5** were obtained by vapor diffusion of Et_2O into a solution of **5** in minimal DCM. Anal. Calcd for $C_{22}H_{36}Cl_2FeP_2Zn$: C, 47.64; H, 6.54. Found: C, 47.59; H, 6.54. $^{31}P\{^1H\}$ NMR ($CDCl_3$): δ −6.78 (s). ^1H NMR ($CDCl_3$): δ 4.55 (s, 4H, Cp), 4.52 (s, 4H, C_5H_4), 2.49 (m, 4H, $-CHMe_2$), 1.50 (dd, $^3J_{H-H} = 7.41$ Hz, $^3J_{H-P} = 15.84$ Hz, 12H, $-CH_3$), 1.39 (dd, $^3J_{H-H} = 7.32$ Hz, $^3J_{H-P} = 15.01$ Hz, 12H, $-CH_3$). $^{13}C\{^1H\}$ ($CDCl_3$): δ 73.33 (t, $^2J_{C-P} = 3.84$ Hz), 71.74 (t, $^3J_{C-P} = 2.31$ Hz), 69.32 (t, $^1J_{C-P} = 15.75$ Hz), 24.56 (t, $^1J_{C-P} = 8.46$ Hz), 19.68 (t, $^2J_{C-P} = 2.31$ Hz), 19.12 (s).

[$CdCl_2$(dippf)] (6). $CdCl_2$ (0.1833 g, 1.00 mmol) was dissolved in 40 mL of 2-propanol−methanol (2:1 v/v). A warm 2-propanol solution (40 mL) of dippf (0.4183 g, 1.00 mmol) was added, and the resulting mixture was refluxed for 2 h. The reaction was allowed to cool to room temperature, during which time an orange solid precipitated. The solution was filtered, and the solid was washed with ether (2 × 5 mL) and dried in vacuo, yielding **6** as an orange solid (0.5026 g, 84%). Anal. Calcd for $C_{22}H_{36}CdCl_2FeP_2$: C, 43.92; H, 6.03. Found: C, 43.89; H, 6.05. $^{31}P\{^1H\}$ NMR ($CDCl_3$): δ 9.61 (s, $^1J_{P-Cd} = 1450$ Hz, $^1J_{P-Cd} = 1390$ Hz). ^1H NMR ($CDCl_3$): δ 4.59 (s, 4H, Cp), 4.42 (s, 4H, C_5H_4), 2.47 (m, 4H, $-CHMe_2$), 1.42 (m, 24H, $-CH_3$). $^{13}C\{^1H\}$ ($CDCl_3$): δ 73.40 (t, $^2J_{C-P} = 5.00$ Hz), 71.29 (t, $^3J_{C-P} = 3.07$ Hz), 68.23 (t, $^1J_{C-P} = 15.0$ Hz), 23.79 (t, $^1J_{C-P} = 7.69$ Hz), 18.65 (s), 18.32 (t, $^2J_{C-P} = 2.31$ Hz).

[$HgCl_2$(dippf)] (7). $HgCl_2$ (0.0478 g, 0.176 mmol) and dippf (0.0736 g, 0.176 mmol) were added to 150 mL of refluxing ethanol. The resulting yellow solution was concentrated to ca. 30 mL by removing the reflux condenser and allowing the solvent to boil off under a strong flow of argon. The hot solution was filtered and the filtrate placed in a freezer overnight. The solution was filtered, and the solid was washed with ether (2 × 5 mL) and dried under vacuum to afford **7** as a yellow powder (0.0294 g, 24%). Anal. Calcd for $C_{22}H_{36}Cl_2FeHgP_2$: C, 38.30; H, 5.26. Found: C, 38.24; H, 5.22. $^{31}P\{^1H\}$ NMR ($CDCl_3$): δ 40.11 (s, $^1J_{P-Hg} = 4190$ Hz). ^1H NMR ($CDCl_3$): δ 4.60 (s, 4H, Cp), 4.47 (s, 4H, C_5H_4), 2.65 (m, 4H, $-CHMe_2$), 1.47 (m, 24H, $-CH_3$). $^{13}C\{^1H\}$ ($CDCl_3$): δ 74.54 (t, $^2J_{C-P} = 4.61$ Hz), 72.34 (t, $^3J_{C-P} = 3.07$ Hz), 26.29 (t, $^1J_{C-P} = 9.99$ Hz), 19.35 (s), 18.96 (s).

[Au_2Cl_2(dippf)] (8). $S(CH_2CH_2OH)_2$ (1.6 mL, 16.47 mmol) dissolved in methanol (3.0 mL) was slowly added to a solution of $HAuCl_4\cdot H_2O$ (0.4484 g, 1.32 mmol) in DI H_2O (3.0 mL) and methanol (14.9 mL) at 0 °C. The resulting mixture was allowed to stir for 15 min. A solution of dippf (0.2254 g, 1.8 mmol) dissolved in $CHCl_3$ (22.4 mL) was slowly added to this mixture and the reaction stirred for 4 h while slowly warming to room temperature. Methanol (50 mL) was added to the reaction, and then the solution was concentrated under vacuum to ca. 30 mL. The reaction was placed in a freezer overnight, and an orange precipitate formed. The solvent was removed by

(9) LeSuer, R.; Geiger, W. E. *Angew. Chem., Int. Ed.* **2000**, *39*, 248.

Table 1. Crystal Data and Structure Analysis Results

	[$PtCl_2$(dippf)]	[$ZnCl_2$(dippf)]
formula	$C_{24}H_{36}Cl_2FeP_2Pt$	$C_{22}H_{36}Cl_2FeP_2Zn$
fw	684.29	554.57
cryst syst	orthorhombic	orthorhombic
space group	Pnna	Pbca
a, Å	16.0504(16)	17.173(4)
b, Å	16.9112(18)	17.134(4)
c, Å	8.8811(10)	17.322(4)
α, deg	90	90
β, deg	90	90
γ, deg	90	90
V, Å^3	2410.6(4)	5097(2)
Z	4	8
cryst size, mm	0.20 × 0.20 × 0.20	0.40 × 0.40 × 0.30
cryst color	orange	orange
radiation; *λ*, Å	0.71073	0.71073
temp, K	220(2)	220(2)
θ range, deg	2.41−28.31	2.05−28.33
data collected		
h	−21 to +21	−20 to +22
k	−21 to +22	−21 to +22
l	−11 to +10	−22 to +22
no. of data collected	16 919	36 429
no. of unique data	2698	6261
abs corr	SADABS	SADABS
final *R* indices (obsd data)		
R1	0.0315	0.0319
wR2	0.0779	0.0828
goodness of fit	1.004	1.012

filtration, and the resulting orange powder was washed with ether (2 × 5 mL) and dried under vacuum, yielding **8** as an orange powder (0.2102 g, 46%). Anal. Calcd for $C_{22}H_{36}Au_2Cl_2FeP_2$: C, 29.92; H, 4.11. Found: C, 29.98; H, 3.77. $^{31}P\{^1H\}$ NMR ($CDCl_3$): *δ* 49.46 (s). ^1H NMR ($CDCl_3$): *δ* 4.74 (s, 4H, Cp), 4.49 (s, 4H, C_5H_4), 2.30 (octet, $^3J_{H-H}$ = 6.96, 4H, −C*H*Me$_2$), 1.27 (dd, $^3J_{H-P}$ = 11.54, $^3J_{H-H}$ = 6.96, 12H, −C*H*$_3$), 1.22 (dd, $^3J_{H-P}$ = 10.54, $^3J_{H-H}$ = 6.96, 12H, −C*H*$_3$). $^{13}C\{^1H\}$ ($CDCl_3$): *δ* 74.97 (s, br), 73.45 (s, br), 25.52 (d, $^1J_{C-P}$ = 35.4 Hz), 19.43 (s).

X-ray Crystallography. Orange-colored crystals of **3** and **5** were mounted on glass fibers with Paratone N oil and then cooled to −53 °C in a stream of nitrogen gas. The data were collected using a Bruker P4/CCD diffractometer with an Apex detector with Mo Kα radiation. Crystallographic data are collected in Table 1. The structures were solved by direct methods and completed from subsequent difference Fourier syntheses. The diffraction symmetry of both compounds indicated orthorhombic crystal systems with space groups of *Pnna* for **3** and *Pbca* for **5**. Absorption corrections to the data were made using the SADABS program. All non-hydrogen atoms were refined anisotropically, and all hydrogen atoms were placed in calculated positions and their isotropic thermal parameters were set to 1.2 or 1.5 times that of the connecting atom. In the case of **3** residual electron density was found for four peaks (1.61, 1.60, 1.51, 1.37 e/Å^3) all within 1 Å of the Pt atom. All programs used in the structural determination and refinement are part of the SHELXL package and can be found in the Bruker AXS computer library (Madison, WI).

Electrochemistry. Electrochemical measurements were conducted using a Princeton Applied Research 263-A potentiostat. The solutions were kept under a blanket of argon for the duration of the experiments. The 1.5 mm diameter glassy carbon working electrode was polished with 1 *μ*m diamond paste, rinsed with acetone, polished with 0.25 *μ*m diamond paste, and washed with DCM prior to use. A platinum wire served as the counter electrode and a nonaqueous silver/silver chloride electrode as the reference electrode. The electrochemical potentials were collected and analyzed using Power Suite from Princeton Applied Research. Simulations were performed using DigiSim.

The oxidative electrochemistry of dippf was investigated in DCM containing 0.050 M $[NBu_4]^+[B(C_6F_5)_4]^-$ as the supporting electrolyte. Analyte concentrations were 0.50, 1.0, and 5.0 mM, and the scan rates employed were from 10 to 1000 mV/s. Electrochemical data were collected at −10, 0, and 10 °C for each analyte concentration. A jacketed cell connected to a temperature-controlled circulating bath was used to maintain the temperature of the solution to within 0.1 °C. The electrochemistry of compounds **1**−**8** was also investigated in DCM with 0.10 M $[NBu_4]^+[PF_6]^-$ as the supporting electrolyte, in which case the concentration of the analyte was 1.0 mM for all of the compounds, and the data were collected at ambient temperature. Decamethylferrocene was added as an internal standard near the end of all the experiments, and the analyte potential was referenced to ferrocene by subtracting 0.62 V.[10]

Results and Discussion

Seven new compounds of dippf were prepared in reasonable yields and thoroughly characterized. Compounds **1** and **4** were determined to be paramagnetic, as anticipated since the dppf analogues of these compounds are also paramagnetic.[8] The Evans method was used to determine a magnetic moment of 3.1 μ_B for compound **1** and 4.6 μ_B for compound **4**.[11] The magnetic moment of **1** is smaller than that of [$NiCl_2$(dppf)], while the magnetic moment of **4** is slightly larger than [$CoCl_2$(dppf)].[8] Both compounds **1** and **4** display magnetic moments within the range expected for Ni(II) and Co(II) in a pseudo-tetrahedral geometry.[12] To characterize these compounds further, the UV−visible spectra were obtained. There are three peaks in the spectrum of compound **1** and four peaks in the spectrum of **4**. While the number of peaks and extinction coefficients are similar to the dppf analogues, the positions of the peaks are slightly different.[8] All of the peaks of **1** occur at lower wavenumbers (approximately 15 nm) than the peaks in [$NiCl_2$(dppf)]. However, there is not a general pattern resulting from a comparison of **4** and [$CoCl_2$(dppf)]; one of the peaks is lower by 10 nm, one is the same, and two are higher by approximately 10 nm.

The new diamagnetic compounds, **3** and **5**−**8**, were characterized by $^{31}P\{^1H\}$, $^{13}C\{^1H\}$, and ^1H NMR. The $^{31}P\{^1H\}$ signal for coordinated dippf is downfield that of the free phosphine for all of the metal centers used in this study with the exception of Zn. For the group 12 metal compounds, the ^{31}P NMR signal for dippf shifts further downfield going down the group. The dppf analogues also show an upfield shift due to coordination of zinc and a trend of the ^{31}P signals shifting downfield going from zinc to mercury.[8] This is opposite the trend in group 6 metal carbonyl compounds containing dppf where the Cr compounds are the furthest downfield.[13] The $^{31}P-^{195}Pt$ and $^{31}P-^{199}Hg$ coupling constants observed for compounds **3** and **7** are similar to the dppf analogues; unfortunately, $^{31}P-^{111}Cd$ and $^{31}P-^{113}Cd$ coupling constants for the dppf analogue were not reported.[8]

In preparing these new compounds, crystals of **3** and **5** suitable for X-ray analysis were obtained. In both

(10) Camire, N.; Mueller-Westerhoff, U. T.; Geiger, W. E. *J. Organomet. Chem.* **2001**, *637*−*639*, 823.

(11) Girolami, G. S.; Rauchfuss, T. B.; Angelici, R. J. *Synthesis and Technique in Inorganic Chemistry*, 3rd ed.; University Science Books: Sausalito, CA, 1999; p 117.

(12) Miessler, G. L.; Tarr, D. A. *Inorganic Chemistry*, 2nd ed.; Prentice Hall: Upper Saddle River, NJ, 1999; p 315.

(13) Hor, T. S. A.; Phang, L.-T. *J. Organomet Chem.* **1989**, *373*, 319.

Table 2. Reversibility and Second-Order Rate Constants for the Oxidation of dippf and dppf

	−10 °C	0 °C	10 °C
reversibility (i_r/i_f) for dippf			
0.50 mM	0.70	0.68	0.65
1.0 mM	0.61	0.57	0.54
5.0 mM	0.51	0.47	0.45
reversibility (i_r/i_f) for dppf			
0.50 mM	0.91[a]	0.88[a]	0.83[a]
rate constant [$10^2 k_D$ (M^{-1} s^{-1})]			
exptl	1.3(0.5)	2.2(0.7)	2.6(1.0)
simulated	1.4(0.1)	2.1(0.1)	3.0(0.2)

[a] Reference 7b.

Table 3. Oxidation Potentials for dippf and Compounds 1−8

compound	E_p (V vs $Fc^{0/+}$)	ΔE_{Fe} (V)	i_r/i_f at 100 mV/s
dippf	0.05		
[$NiCl_2$(dippf)] (**1**)	0.33	0.28	0.70
[$PdCl_2$(dippf)] (**2**)	0.43	0.38	1.05
[$PtCl_2$(dippf)] (**3**)	0.48	0.43	1.02
[$CoCl_2$(dippf)] (**4**)	0.33	0.28	1.07
[$ZnCl_2$(dippf)] (**5**)	0.37	0.32	
[$CdCl_2$(dippf)] (**6**)	0.45	0.40	0.59
[$HgCl_2$(dippf)] (**7**)	0.50, 0.66		0.69, 1.02
[Au_2Cl_2(dippf)] (**8**)	0.54	0.49	1.00

Table 4. Selected Bond Angles (deg) and Lengths (Å) for [MCl_2(dippf)]

	3	**5**
M	Pt	Zn
P−M−P	103.78(5)	109.98(2)
Cl−M−Cl	85.51(6)	109.62(3)
X_A−Fe−X_B[a]	179.83[e]	177.24[e]
P−Fe−P	63.02[e]	70.90[e]
τ[b]	34.8[e]	48.5[e]
θ[c]	3.7	3.3
av P−M	2.2666	2.4153
av M−Cl	2.3548	2.2526
av Fe−C	2.030	2.0490
P−P	3.567[e]	3.957[e]
av δ_P[d]	0[e]	0.0072[e]

[a] Centroid−Fe−centroid. [b] The torsion angle C_A−X_A−X_B−C_B where C is the carbon bonded to the P and X is the centroid. [c] The dihedral angle between the two Cp rings. [d] Deviation of the P atom from the Cp plane, a positive value meaning the P is closer to the Fe/Ru. [e] Determined from the structural data using ORTEP-3 for Windows.[29]

structures, the dippf ligand adopts a synclinal staggered arrangement in which the phosphorus atoms are gauche and the Cp rings are staggered (Table 4).[1,14] This is the most common arrangement for the Cp rings of dppf when it is bonding as a chelate ligand.[1,14] An analysis of the reported dippf structures indicates that synclinal staggered is the only conformation reported for compounds containing a chelating dippf ligand.[5]

The platinum center of **3** is pseudo-square-planar (Figure 1). Compared to the corresponding angles in **2**, the P−Pt−P angle is only 0.21° larger while the Cl−Pt−Cl angle is 2.04° smaller.[2] This is significantly different from the dppf analogues, where the P−Pt−P angle is 1.3° larger and the Cl−Pt−Cl is 3.7° smaller than the corresponding angles in the Pd compounds.[15] In addition, the P−M−P angles in **2** and **3** are approximately 4.5° larger than in the dppf analogues. This suggests that the bulkier isopropyl groups of dippf, as compared to the phenyl groups of dppf, maximize the bite angle of the phosphine in bonding to Pd and Pt. The influence of the bite angle of dippf and dppf has been noted in the reactivity of [PdMe(CH_3CN)(P⌒P)]$^+$ (P⌒P = dppf or dippf).[16]

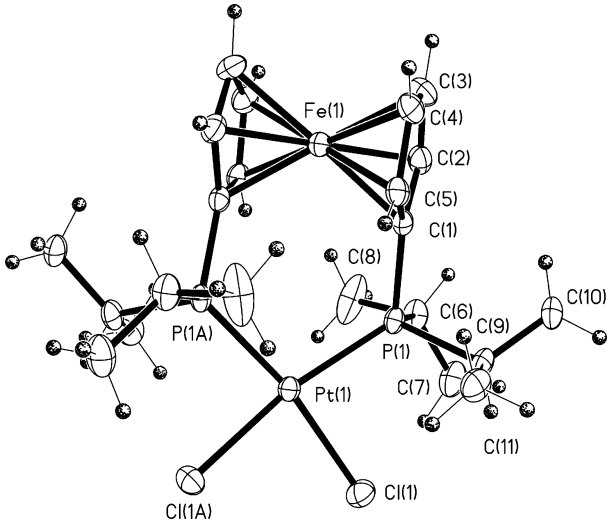

Figure 1. ORTEP diagram of [$PtCl_2$(dippf)].

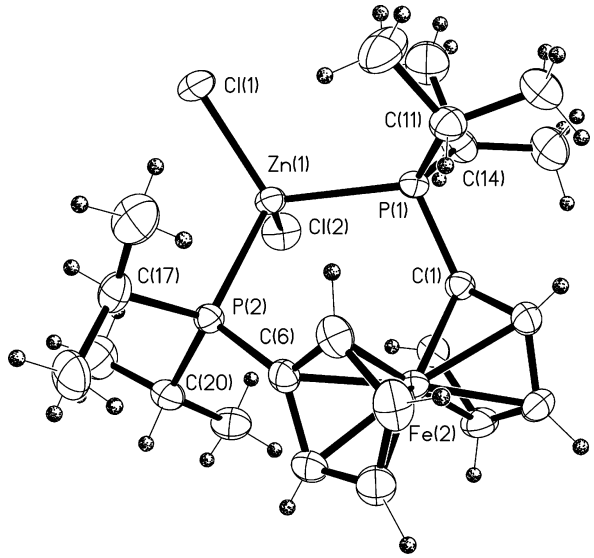

Figure 2. ORTEP diagram of [$ZnCl_2$(dippf)].

In compound **5**, the Zn center adopts a pseudo-tetrahedral geometry (Figure 2). The structure of the dppf analogue has not been reported. However, the geometry was presumed to be pseudo-tetrahedral.[8] The structure of **5** is the first containing zinc with a chelating diphosphine ligand. However, there are a number of structures in which Cd and Hg are bound to chelating phosphines including [$CdBr_2$(dppf)],[17] [$HgCl_2$(dppf)],[18] and [HgI_2(dppf)].[19] As with compound **5**, the group 12

(14) Bandoli, G.; Dolmella, A. *Coord. Chem. Rev.* **2000**, *209*, 161.
(15) (a) Hayashi, T.; Konishi, M.; Kobori, Y.; Kumada, M.; Higuchi, T.; Hirotsu, K. *J. Am. Chem. Soc.* **1984**, *106*, 158. (b) Clemente, D. A.; Pilloni, G.; Corain, B.; Longato, B.; Tiripicchio-Camellini, M. *Inorg. Chim. Acta* **1986**, *115* L9.
(16) Zuideveld, M. A.; Swennenhuis, B. H. G.; Kamer, P. C. J.; van Leeuwen, P. W. N. M. *J. Organomet. Chem.* **2001**, *637−639*, 805.
(17) Wang, X.-L.; Huang, Z.-X.; Liu, S.-X. *Jiegou Huaxue* **2001**, *20*, 486.
(18) McGinley, J.; McKee, V.; McKenzie, C. J. *Acta Crystallogr., Sect. C: Cryst. Struct. Commun.* **1998**, *54*, 345.
(19) Niu, Y. Y.; Song, Y.-L.; Liu, S.-X.; Xin, X.-Q. *Z. Anorg. Allg. Chem.* **2002**, *628*, 179.

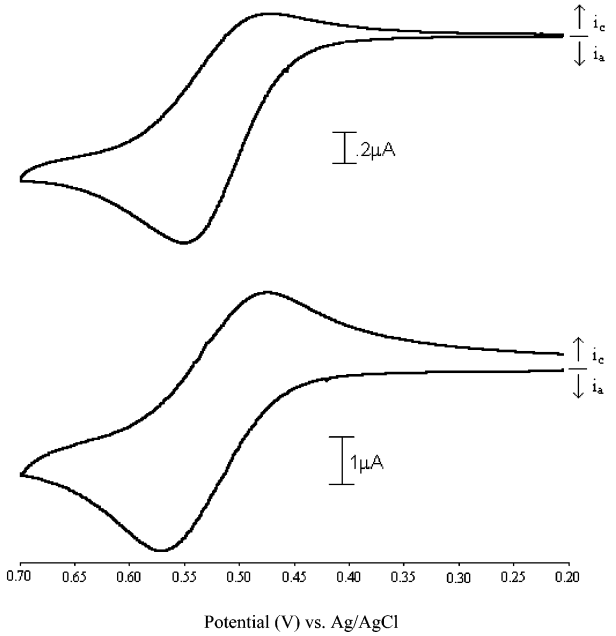

Figure 3. CV scans of the oxidation of 1.0 mM dippf in DCM/0.05 M $[NBu_4]^+[B(C_6F_5)_4]^-$ at 263 K at two different scan rates: (top) 10 mV/s; (bottom) 75 mV/s.

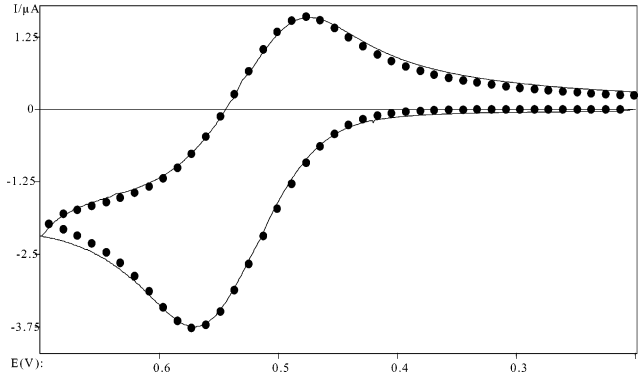

Figure 4. Comparison of experimental (—) and simulated (●) cyclic voltammogram for oxidation of dippf in DCM at 263 K with concentration 1.00 mM and $\nu = 100$ mV/s. Simulation parameters were $E_{1/2} = 0.520$ V, $k_s = 1.0$ cm/s, $1 - \alpha = 0.5$, dimerization $K_{eq} = 1 \times 10^6$, $k_{D(17)} = 200$ (M^{-1} s^{-1}), $R_u = 5000$, $C_{dl} = 0.0$ μF.

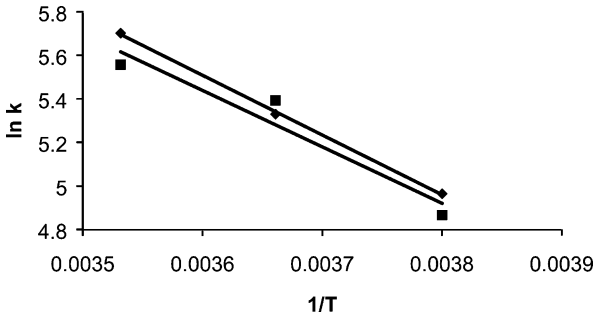

Figure 5. Arrehenius plot of experimental (■) and simulated (◆) data. For the experimental data slope $= -2.59 \times 10^3$, intercept $= 14.8$, and $R^2 = 0.9276$ and for the simulated data the slope $= -2.75 \times 10^3$, intercept $= 15.4$, and $R^2 = 0.9993$.

metal in the dppf compounds is pseudo-tetrahedral, and the dppf ligand is synclinal staggered.

The oxidative electrochemistry of dippf at various concentrations and temperatures shows a chemically reversible wave (Figure 3). The electrochemical parameter, E_L(L) has been defined as $1/2E°$ (Fe^{III}/Fe^{II}) (vs NHE) for symmetric ferrocenes and can be used to estimate the effect of Cp ring substitution on the $E_{1/2}$ of the ferrocene.[20] For dippf, E_L(L) has been determined to be 0.36 V. For ferrocene compounds, the E_L(L) can be estimated using the equation $E_L(\text{calc}) = 0.45\sigma_p + 0.36$, where σ_p is the Hammett substituent constant for the functional group on ferrocene.[20] For the $-P(i\text{-}Pr)_2$ group, the σ_p is 0.06,[21] giving an E_L(calc) of 0.39 V, which is in reasonable agreement with the experimental value.

The reversibility of the oxidation of dippf is dependent on the temperature, scan rate, and analyte concentration, and under appropriate conditions, a reversible couple is observed. At scan rates below 300 mV/s, the oxidation of dippf appears be coupled to a chemical follow-up reaction: an EC mechanism.[22] Although the product of this reaction could not be isolated, the data suggest a second-order reaction. On the basis of previous work on the dppf analogue[7] as well as the dependence of the electrochemical response on the analyte concentration and simulations (see below) we propose the chemical step to be a dimerization, EC_{dim}. Since the dimerization can be complicated by reacting with the supporting electrolyte,[7a] the weakly coordinating $[NBu_4]^+[B(C_6F_5)_4]^-$ was used as the supporting electrolyte.[9,10,23] The chemical reversibility parameter (i_r/i_f) for this electrochemical dimerization was calculated at all concentrations and temperatures employed in this study.[24] The values obtained at a scan rate of 50 mV/s are shown in Table 2. The smaller current ratios for dippf as compared to dppf suggest that the dippf cation is less stable and forms the dimer more rapidly than dppf under similar conditions.[7]

The second-order rate constant for the dimerization reaction (k_D) was calculated using the values of i_r/i_f.[25] For each temperature, average values of k_D along with the average deviations from the mean were determined and are shown in Table 2. DigiSim was used to simulate the experimental data, and a dimerization mechanism gave a good fit of the experimental data (Figure 4). The experimental and simulated values of k_D can be related to activation parameters through an Arrhenius relationship (Figure 5). The experimental values obtained for $\Delta H^‡$ and $\Delta S^‡$ were 19(1) kJ/mol and −220(10) J/mol·K, and the simulated values were 20(1) kJ/mol and −220(10) J/mol·K, respectively. The entropy of activation for the electrochemical dimerization of dippf is identical to that of dppf; however, the enthalpy of activation is approximately 6 kJ/mol lower.[7] It is difficult to account for the differences in the enthalpy of activation values for the electrochemical dimerization of dppf and dippf. One possible factor is the size of a

(20) Lu, S.; Strelets, V. V.; Ryan, M. F.; Pietro, W. J.; Lever, A. B. P. *Inorg. Chem.* **1996**, *35*, 1013. From this reference, $F_c = 0.66$ V vs NHE.

(21) Hansch, C.; Leo, A.; Taft, R. W. *Chem. Rev.* **1991**, *91*, 165.

(22) Geiger, W. E. In *Laboratory Techniques in Electroanalytical Chemistry*, 2nd ed.; Lissinger, P. T., Heineman, W. R., Eds.; Marcel Dekker: New York, 1996; p 683.

(23) Camire, N.; Nafady, A.; Geiger, W. E. *J. Am. Chem. Soc.* **2002**, *124*, 7260.

(24) Olmstead, M. L.; Hamilton, R. G.; Nicholson, R. S. *Anal. Chem.* **1969**, *41*, 260.

(25) Lasia, A. *J. Electroanal. Chem.* **1983**, *146*, 413.

phenyl group in comparison to an isopropyl group. This has been seen in the kinetic stability of triarylphosphonium radical cations, which is influenced by the steric bulk of the aryl groups.[26] A second possible factor is interaction of the unpaired electron with the delocalized π-system in dppf, which is not possible in dippf. It is also possible that differences in the solvation of the radical cations are responsible for the difference in activation enthalpy. Additional studies of these types of systems will provide greater insight into this interesting observation.

Upon coordination, the ferrocene-based oxidation of dippf shifts to more positive potentials (Table 3). A similar trend has been noted for the dppf analogues of compounds **2**, **3**, and **8**.[7b,8] Coordination eliminates dimerization as a possible chemical pathway following oxidation of the dippf moiety, and it appears that decomposition of the cation is slow on the CV time scales used in this study. However, similar to the oxidation of the dppf analogues,[8] oxidation of compounds **1**, **4**, and **6** is chemically reversible. The oxidation of compound **5** is irreversible. For $[MCl_2(dppf)]$ (M = Zn or Cd), the instability of the oxidized species has been attributed to the weakening of the purely σ P→M bond due to oxidation of the iron center.[8] The P→M bond is anticipated to be stronger in compounds **5** and **6**, as alkyl groups make phosphines more basic and therefore more donating than phenyl groups.[27] The anticipated stabilization due to the isopropyl groups appears to be minimal, as the products from oxidation of compounds **5** and **6** are highly reactive. Compound **7** displays two oxidation waves. The first wave is irreversible, while the second wave is reversible. The report of the electrochemistry of the dppf analogue of **7** reports that the oxidation is irreversible due to weakening of the σ P→M bond.[8] The $[MCl_2(dippf)]^+$ (M = Pd or Pt) species are stable on the time scales of this study based on the reversibility of the oxidation wave. A similar observation was made for the dppf analogues, and the stability was attributed to M→P back-donation from the square-planar metal center.[8] It is unclear why **1** and **4** do not form stable oxidation products. The pseudo-tetrahedral coordination environment of the central metal may not stabilize the oxidation product, as seen in compounds **5**−**7**.

The difference between the oxidation potential of uncoordinated dippf and the compounds containing a coordinated dippf ligand can be defined as ΔE_{Fe}. For the group 10 metals, the square-planar Pd and Pt compounds exhibit similar ΔE_{Fe} values, which are significantly larger than the ΔE_{Fe} for the tetrahedral $[NiCl_2(dippf)]$. This has also been noted in the dppf and dppr (dppr = 1,1′-bis(diphenylphosphino)ruthenocene) analogues.[7b,8] The ΔE_{Fe} for **1** (0.28 V) is significantly larger than the ΔE_{Fe} for $[NiCl_2(dppf)]$ (0.07 V) and the ΔE_{Ru} for $[NiCl_2(dppr)]$ (0.15 V), while the values for **2** (0.38 V) and **3** (0.43 V) are similar to the ΔE_{Fe} of the dppf analogues (0.39 V) and the ΔE_{Ru} for the corresponding dppr compounds (0.52 V).[7b,8]

The ΔE_{Fe} for the tetrahedral compound **1** is different from the ΔE_{Fe} values for the square-planar compounds **2** and **3**, which are identical. While the structures may play an important part in this phenomenon, similar trends were noted for the other compounds in this study. In general, the ΔE_{Fe} for dippf bound to a 3d metal is approximately 0.29 V, while the ΔE_{Fe} is approximately 0.42 V for dippf bound to either a 4d or 5d metal. This implies that the first wave seen for the oxidation of **7** is likely to be ferrocene-based. It was anticipated that going down a group, the ΔE_{Fe} would decrease due to the increased electron density at the metal center.[27] This general trend has been noted in the oxidation potentials of $(OC)_5M(\mu\text{-dppf})AuCl$ (M = Cr, Mo, or W), which are less positive going down group 6.[28] However, the same authors report the oxidation potentials for $(OC)_5M(\mu\text{-dppf})M'Cl_2$ (M = Cr, Mo, or W; M′ = Pd or Pt) and for Pd and Pt.[28] The tungsten analogue has the most positive oxidation potential and the molybdenum the least. An explanation for the general trend observed for the dippf compounds is not apparent.

Conclusion

The electrochemical oxidation of dippf has an oxidation potential of 0.01V vs $Fc^{0/+}$. The oxidation of dippf follows an EC mechanism with the chemical follow-up reaction being a dimerization, similar to the related compound, dppf.[7] In comparing the activation parameters for these dimerization reactions, the entropy of activation values are identical, but the enthalpy of activation of dppf is approximately 6 kJ/mol larger. This difference may be due to stabilization of the phosphonium radical cation by the bulkier isopropyl groups of dippf.

Seven new compounds containing dippf were prepared in good yield and characterized spectroscopically. In addition, the X-ray structures of $[MCl_2(dippf)]$ (M = Pt or Zn) were obtained. The structure of $[ZnCl_2(dippf)]$ is the first reported structure of a chelate phosphine bound to a zinc center. As anticipated, the zinc is in a pseudo-tetrahedral coordination environment.[8]

The oxidative electrochemistry of the new dippf compounds and the previously reported $[PdCl_2(dippf)]$ was investigated. The oxidation potentials of the compounds are more positive than that of free dippf. In general, the oxidation potentials of the compounds containing a 3d metal are less positive than those of 4d and 5d metals.

Acknowledgment. C.N. and J.O. thank the Academic Research Committee (Lafayette College) for its support through an EXCEL scholarship, the donors of the Petroleum Research Fund, administered by the American Chemical Society, for partial support of this research, and the Kresge Foundation for the purchase of the JEOL Eclipse 400 MHz NMR.

Supporting Information Available: Tables of crystal data collection and refinement parameters, bond distances and angles, and anisotropic displacement parameters for **3** and **5**. This material is available free of charge via the Internet at http://pubs.acs.org.

OM0340138

(26) Culcasi, M.; Berchadsky, Y.; Gronchi, G.; Tordo, P. *J. Org. Chem.* **1991**, *56*, 3537.
(27) Angelici, R. J. *Acc. Chem. Res.* **1995**, *28*, 51.
(28) Phang, L.-T.; Au−Yeung, S. C. F.; Hor, T. S. A.; Khoo, S. B.; Zhou, Z.-Y.; Mak, T. C. W. *J. Chem. Soc., Dalton Trans.* **1993**, 165.
(29) Farrugia, L. J. *J. Appl. Crystallogr.* **1997**, *30*, 565.